(27) Flory, P. J. *Principles of Polymer Chemistry*; Cornell University Press: Ithaca NY, 1953; Chapter IX, pp 354-356.
(28) Flory, P. J. *J. Am. Chem. Soc.* **1941**, *63*, 3083, 3091, 3097.
(29) Ross-Murphy, S. B. *J. Polym. Sci., Polym. Symp.* **1975**, *No. 53*, 11-22.
(30) Ross-Murphy, S. B. Ph.D. Thesis, Essex University, 1974.
(31) Stepto, R. F. T. *Faraday Discuss. Chem. Soc.* **1974**, *57*, 69.
(32) Shultz, A. R. *J. Am. Chem. Soc.* **1958**, *80*, 1854.

Surfactant-Free Emulsion Polymerizations: Predictions of the Coagulative Nucleation Theory

P. John Feeney, Donald H. Napper, and Robert G. Gilbert*

School of Chemistry, The University of Sydney, Sydney, N.S.W. 2006, Australia.
Received September 22, 1986

ABSTRACT: Equations are set down for the formation of latex particles in emulsion polymerization systems in the absence of added emulsifier. The model describes the formation of colloidally unstable precursor particles through homogeneous nucleation, followed by their coagulation and propagational growth to form colloidally stable latex particles. Coagulation rates are obtained through DLVO theory and its modifications, with due allowance for the partial attraction that occurs in the coagulation between particles with different radii. Calculations show good agreement with the experimental data of Ottewill and co-workers for the variation of particle number density with initiator concentration and ionic strength.

Introduction

The mechanisms whereby polymer latex particles are formed in heterogeneous polymerization systems, both in the presence and absence of added surfactant, remain a matter for active investigation. At least three theories have been proposed to account for particle nucleation in heterophase polymerizations: the entry of free radicals into micelles,[1,2] homogeneous nucleation resulting from the precipitation of growing oligomers,[3-7] and the coagulative nucleation of precursor particles (subsequent to their formation by homogeneous nucleation).[4,8-12] The results of recent experimental determinations[12] of the time evolution and the size distributions of the latex particles formed in a conventional styrene emulsion polymerization appear to be in qualitative and quantitative conflict with the predictions of any single-step nucleation mechanism, including both micellar entry and simple homogeneous nucleation. These results are, however, in conformity with the predictions of the multistep nucleation mechanism postulated to be operative in the coagulative nucleation theory.[12] This theory is also consistent with the observation of periodic nucleation phenomena (Liesegang rings) in certain polymerizing systems.[13]

It has long been known that stable latex particles can also be generated in emulsifier-free systems, even with monomers such as styrene that are comparatively insoluble in water, provided that the initiator decomposition gives rise to charged primary free radicals. In such systems, the possibility of particle nucleation occurring by a micellar entry mechanism is virtually precluded. Although the micellization of the oligomeric surfactant molecules generated in situ in these systems has been postulated,[14] there is no experimental evidence even to hint at its occurrence. In these surfactant-free systems, coagulative nucleation appears to be significant in particle formation, as Ottewill and co-workers were the first to highlight.[9,10] These workers determined experimentally the effects of varying the ionic strength and the initiator concentration on the mean size of the latex particles formed. Their results were qualitatively in accord with the expectations of a coagulative nucleation mechanism.

A primitive theoretical treatment of coagulative nucleation has been presented previously.[12] It is worthwhile to examine the application of the model to systems in which there is no added surfactant. The precise experimental results of Ottewill and co-workers[10] for persulfate-initiated styrene systems provide a benchmark against which the quantitative predictions of the theory can be compared. The current paper gives a considerable development of the theory presented earlier,[12] as well as correcting some errors therein.

In coagulative nucleation, the basic mechanistic assumption is that the coagulation of "precursor" particles is involved in the formation of mature latex particles. These precursors are small (say, less than 5 nm in radius) and differ from true latex particles in two important respects. First, precursors are colloidally unstable. Second, precursor particles imbibe only relatively small amounts of monomer when compared with mature latex particles; thus, while growth occurs both by aggregation and propagation, the former must be important for smaller precursors. Both of these properties of precursors arise from the high curvature of their surfaces. Each precursor particle is composed of one or more primary precursor particles, the latter being formed by the propagational events that primary free radicals undergo in the aqueous phase after being generated by initiator decomposition. The particular character of the primary precursors is presumed to arise from oligomeric species whose chain lengths exceed the critical degree of polymerization required for solubility in the aqueous phase, i.e., homogeneous nucleation.

Coagulative Nucleation Theory

The coagulative nucleation theory calculates the rate of particle formation from (i) the rate of homogeneous nucleation and formation of primary precursors, based on the Hansen-Ugelstad-Fitch-Tsai (HUFT) theory;[7] (ii) the kinetics of coagulation among precursor particles, using the Smoluchowski-Müller-Fuchs theory, with the coagulation rate coefficients being calculated employing DLVO theory,[15] modified as required for heterocoagulation; and (iii) propagational growth.

Let Y_i be the number concentration of precursor particles with swollen volume $V_i = iV_p$, where V_p is the volume of a newly formed primary precursor particle. The pop-

0024-9297/87/2220-2922$01.50/0

ulations of precursor particles change as a result of coagulation (when a particle of volume V_{i+j} is formed by agglomeration of particles with volumes V_i and V_j) and by propagation. This leads to the population balance equations:

$$dY_j/dt = \sum_{i=1}^{j/2} B_{i,j-i}Y_iY_{j-i} - Y_j\sum_{i=1}^{m} B_{ij}Y_i + G_{j-1}Y_{j-1} - G_jY_j + g(t)\delta_{j1} \quad (1)$$

$$dY_m/dt \equiv dN_c/dt = \sum_{i=1}^{m-1}\left(\sum_{j=j_{min}}^{m-1} B_{ij}Y_iY_j\right) + G_{m-1}Y_{m-1} \quad (2)$$

Here B_{ij} is the rate coefficient for coagulation between precursors with volumes V_i and V_j, G_j is the rate of volume growth by propagation for a precursor with volume V_j, j_{min} is the larger of i and $m - i$, and V_m denotes the volume at which precursors become true latex particles, i.e., colloidally stable. Thus Y_m is identically the number concentration of latex particles, N_c. The term $g(t)$ is the rate of formation of primary precursors by homogeneous nucleation (as quantified below); $\delta_{ij} = 0$, $i \neq j$; $\delta_{ij} = 1$, $i = j$. The summation limits in eq 1 and 2 are such as to avoid double counting of various events; note that if j is odd, the upper limit for the first summation in eq 1 is $(j/2 - {}^1/_2)$. Equation 1 corrects some minor errors in our earlier work.[12] The volume of each type of precursor (i.e., $j < m$) is by definition constant, and thus for $j < m$, the G_j are given by

$$G_j = \bar{n}k_pC_M{}^jM_0/(N_Ad_pV_p) \qquad (j < m) \quad (3)$$

where $\bar{n}$ is the average number of free radicals per precursor particle, k_p is the propagation rate coefficient, $C_M{}^j$ is the monomer concentration inside a precursor with volume V_j, M_0 is the molecular weight of monomer, N_A is Avogadro's constant, and d_p the density of polymer. Since the volume of the stable latex particles, V_m, varies in time because of propagational growth and is given by $V_m = mV_p + t\bar{n}k_pC_M{}^mM_0/(N_Ad_p)$, one has $G_{m-1} = G_{m-2}V_p/(V_m - V_{m-1})$.

Equations 1 and 2 are in fact the finite difference forms of the equations for the time evolution of the full particle size distribution. In the limit as V_p is taken to zero, we have for the population of particles with volume V at time t

$$\partial Y/\partial t = \int_0^{V/2} B(V-V',V')Y(V-V')Y(V')\,dV' - Y(V)\int_0^{\infty} B(V,V')Y(V')\,dV' - \frac{\partial}{\partial V}K(V)Y(V) \quad (4)$$

where $K(V) = \bar{n}k_pC_M(V)M_0/(N_Ad_p)$, and eq 4 is to be solved subject to the boundary condition $Y(t,V=0) = g(t)$. Strictly speaking, eq 4 should be replaced by separate equations for the volume distributions of particles containing different numbers of free radicals, so as to take proper account of stochastic broadening, etc. Such a sophistication, while essential to the prediction of the particle size distributions after nucleation has ceased, is not needed to describe nucleation, since coagulation is sufficiently rapid for the distribution of free radicals to remain close to its constant, pseudo-steady-state value.

It is useful to point out that eq 4, which is a general and exact equation for coagulative and propagative growth, sheds light on the question of the precise form of eq 1. Thus, some authors have written eq 1 with the coefficients for the diagonal term ($B_{ii}Y_i{}^2$) differing in some places by a factor of 2 from those given above, and some argument exists in the literature as to what the correct form actually should be. However, it is apparent that eq 1 is in reality a finite difference approximation to the integral relation of eq 4. Thus one may evaluate the integral terms therein (with varying accuracy) as sums either of rectangles or of trapzoids. The forms of eq 1 that differ by the factors of 2 just discussed are precisely these alternative approximations to the integrals. The differences between numerical results obtained from either alternative expression will disappear as the grain size used to evaluate the integrals is taken sufficiently small. Thus in fact it is immaterial which of the alternative expressions one adopts, provided one uses an appropriately small grain size.

We shall return to eq 4 at a later point, to show how the quantity m (giving the volume at which a particle becomes colloidally stable) may be eliminated as a parameter in the calculations.

We next specify $g(t)$, the rate of production of primary precursors by homogeneous nucleation; our development here is a minor extension of the HUFT theory.[7] Let y_P denote the concentration of primary particles (oligomers) of degree of polymerization P. These are created by initiator decomposition, grow by propagation, and disappear (i) by self-termination, (ii) by entry into precursors, and (iii) (for the largest) by forming primary precursors. We define $P = 1$ as corresponding to the primary free radical (e.g., $SO_4{}^{\bullet-}$). We thus obtain the evolution equations

$$dy_P/dt = 2k_dC_I\delta_{1P} - y_P\sum k_t{}^{PP'}y_{P'} - k_p(C_M{}^Py_P - C_M{}^{P-1}y_{P-1}) - y_P\sum B_{Pj}Y_j \quad (5)$$

where the term in $P - 1$ is absent for $P = 1$. Here k_d is the initiator decomposition rate coefficient, C_I is the initiator concentration, $k_t{}^{PP'}$ is the termination rate coefficient between oligomers with degrees of polymerization P' and P, $C_M{}^P$ is the monomer concentration around the free radical in an oligomer with degree of polymerization P, and B_{Pj} is the rate coefficient for entry of a P-meric oligomer into a precursor with volume V_j. The inclusion of termination in eq 5 obviates the need to introduce a free radical capture efficiency. Note that (for a sparingly soluble monomer) $C_M{}^P$ will be a strong function of the degree of polymerization: it must vary from the aqueous phase monomer concentration for small P through to that typical of a precursor for large P.

The rate of creation of primary precursors is then given by

$$g(t) = k_pC_M{}^Jy_J \quad (6)$$

where J (or j_{crit} in the usual HUFT notation) is the degree of polymerization at which an oligomer becomes a primary precursor.

In the limit of large J, eq 5 can be written in a form analogous to eq 4:

$$\partial y(P)/\partial t = -k_p\partial(C_M{}^Py)/\partial P - y\int k_t(P,P')y(P')\,dP' - y\int B(V_P,V)Y(V)\,dV \quad (7)$$

Equation 7 is subject to the boundary condition $y(t,P=1) = 2k_dC_I$.

Now, oligomers are by definition so small in size that their contribution to the final particle number by mutual termination or entry into precursors is negligible. It is then apparent that eq 4 and 7 are really subsets of the same general equation, which gives the overall evolution of the particle size distribution. Thus there is no need to make an artificial distinction between primary oligomers, precursors, and colloidally stable latex particles. Nevertheless, such a distinction (reflecting species for which different terms dominate in the evolution equations) is very convenient. The essential difference between precursors (Y) and oligomers (y) is that the latter are so small that they

have a negligible direct contribution to the particle size distribution. The values of m and J are in fact simply quantities involved in the practical numerical simulation. They can be eliminated as parameters by taking the limits as $m \to \infty$ and $J \to 0$.

Next, we specify the form of the coagulation rate coefficients B_{ij}, using the Fuchs[16] formulation coupled with DLVO theory, modified as required to encompass heterocoagulation:[17-19]

$$B_{ij} = (4/3)(k_B T/\eta W_{ij})(1 + r_i/r_j)^2/(2r_i/r_j) \quad (8)$$

where k_B is Boltzmann's constant, T is the temperature, η is the viscosity of the medium, r_j is the radius of the particle, and W_{ij} is the Fuchs stability ratio, given by

$$W_{ij} = (\kappa r_{ij})^{-1} \exp(E_m/k_B T) \quad (9)$$

Here κ^{-1} is the thickness of the double layer, E_m is the height of the potential barrier that must be surmounted for coagulation to occur, and $r_{ij} = 2r_i r_j/(r_i + r_j)$. The value of κ (in SI units) is given by

$$\kappa = [8\pi^2 N_A I e^2/(4\pi\epsilon k_B T)]^{1/2} \quad (10)$$

where e is the electronic charge, I the ionic strength, and ϵ the permittivity of the dispersion medium. The ionic strength is given by

$$I = \tfrac{1}{2}\sum z_i^2 C_i \quad (11)$$

where z_i is the valence number on the ith species whose concentration is C_i.

E_m can be calculated from the DLVO theory with extensions for heterocoagulation.[19-25] E_m is the maximum in the total potential energy $V = V_A + V_R$, where the latter quantities are respectively the van der Waals attractive and electrostatic repulsive potential.

The calculation of V_R is complicated. For particles whose radii are not greatly different, and provided κr_i and κr_j are both appreciably greater than unity, V_R (in SI units) can be calculated by using an expression due to Hogg et al.[19]

$$V_R(r_i,r_j,H) = \tfrac{1}{2}\pi\epsilon\zeta^2 r_{ij}\left[\frac{2\zeta_i\zeta_j}{\zeta^2}\ln[(1+q)/(1-q)] + \ln(1-q^2)\right] \quad (12)$$

where ζ_i is the ζ-potential of a particle with radius r_i, $\zeta^2 = \zeta_i^2 + \zeta_j^2$, and $q = \exp(-\kappa H)$, with H the closest distance between the surfaces of the particles (the maximization is with respect to this distance). The constant surface charge density form for V_R is used here because the ions determining the potential are actually incorporated into the latex particles.

Equation 12 can become quite inaccurate under certain circumstances.[22,23] One region of inaccuracy of eq 12 is when the particles are highly curved. For, say, $5 \le \kappa r \le 20$, eq 12 may be replaced by[24]

$$V_R(r_i,r_j,H) = 32\pi\epsilon r_{ij}(k_B T/ez)^2\gamma_i\gamma_j q \quad (13)$$

where $\gamma_i = \tanh(ze\zeta_i/4k_B T)$. For $\kappa r < 5$, we commence with the expression for equal spheres[25]

$$V_R(r_j,r_j,H) = 4\pi\epsilon r_j\zeta_j^2 q/(2 + H/r_j)$$

and extend it empirically to encompass spheres of unequal radii by writing

$$V_R(r_i,r_j,H) = 4\pi\epsilon r_{ij}\zeta_i\zeta_j q/(2 + H/r_{ij}) \quad (14)$$

On a technical note, it should be pointed out that eq 12–14 do not give a continuous form for V_R as a function of κr_{ij}. Computationally, it is usually necessary to have a functional form which is continuously differentiable to a fairly high order; this is achieved by having a V_R which is made to be a continuous function of κr_{ij} through use of a switching function: e.g., with eq 13 and 14, we put $V_R = (1 - s_w)V_{14} + s_w V_{13}$, where s_w is a switching function, such that $s_w = \tfrac{1}{2}[1 + \tanh[\tfrac{1}{2}(\kappa r_{ij} - 5)]]$, and V_{13} and V_{14} are the values of V_R computed from eq 13 and 14, respectively. The precise form of the switching function is not important.

A regime where eq 12–14 become inaccurate is particularly important for the present system: when the two particles have very different radii and very different surface potentials.[22] Barouch and Matijevic[22] have cast serious doubts about the validity of eq 12–14 when applied to heterocoagulation of such particles. In particular, we note that these expressions apparently result in a large overestimate of the repulsive barrier for the heterocoagulation of spheres. For example, exact calculations show that the coagulation between particles of the sizes of primary precursors and mature particles (with surface potentials typical of those in the present system) exhibit barriers which are relatively small and are also comparatively insensitive to the ionic strength and surface charge density. This is in contradiction to the predictions of eq 12–14, which give comparatively high barriers that are more strongly sensitive to surface charge and ionic strength. The reason for the difference in these predictions resides in the partial electrostatic attraction that occurs on close approach between two particles of different size and different surface potential, even when the potentials are of the same sign. The theory of Barouch and Matijevic takes this partial attraction into account when calculating the energy barrier to coagulation, whereas the alternative approach does not.

Barouch and Matijevic obviated this problem with eq 12–14 by obtaining more precise solutions of the Poisson–Boltzmann equation.[22,23] However, the implementation of these improved solutions is computationally a major task,[22] so that in practice it cannot be incorporated directly as part of the numerical solution of coupled differential equations. Unfortunately, the breakdown of eq 12–14 cannot be ignored in the present context: as stated above, these equations predict that there will be a significant repulsive barrier between a large particle (such as a mature latex particle) and a small one (such as a primary precursor), whereas the more precise solutions predict a smaller barrier as a result of the partial attraction. Thus the simple application of eq 12–14 grossly underestimates the rate at which mature particles "mop up" the primary precursors when the former become sufficient in number, and so the nucleation period is predicted to be falsely long. The partial attraction between spheres of disparate radius and surface potential thus appears to play an important role in "switching off" the nucleation process in these systems. In the present publication we overcome this difficulty by the following pragmatic approach. If r_i and r_j differ by (say) more than a factor of 2, we replace the B_{ij} calculated by using eq 12–14 by that calculated from the following expression for the potential barrier:

$$E_m/k_B T = (8 \times 10^{10})(1 + 1.4 \times 10^{-9}\,\kappa)r_{ij}\zeta_i\zeta_j \quad (r_i/r_j \ge 2 \text{ or } r_i/r_j \le \tfrac{1}{2}) \quad (15)$$

(where all quantities are in SI units; the units of r_{ij} are thus meters, not nanometers). Equation 15 is a semiempirical relation obtained by fitting the results of a number of calculations of $E_m/k_B T$ obtained by using the method of Barouch et al.[22,23] The calculations from which eq 15 was

obtained were for r_i = 2 nm, r_j over the range 5–6 nm, values of ζ_i over the range 12–20 mV, and of ζ_j over the range 60–80 mV, and κ over the range (3–4.5) × 10^8 m^{-1}; these values are typical for the systems examined in the present paper. Equation 15 fulfills the requirement of allowing larger and smaller particles to coagulate with only a small repulsive barrier, as demanded by the full theory. As long as the incorrect strong repulsion between small and large particles predicted by eq 12–14 is replaced by a physically reasonable value corresponding to a small barrier, the time evolution of the particle number is not strongly influenced by the choice of E_m/k_BT. It is for this reason that we ignore the fact that eq 15 was derived on the basis of constant surface potential rather than constant surface charge density. We note that an important area for future development is a computationally feasible means of incorporating more accurate theories for heterocoagulation into the solution of the nucleation equations.

The ζ-potential used in the foregoing development is calculated from the surface potential by applying the Stern layer correction.[4] One has

$$\zeta = (2k_BT/z_+e) \ln [(e^E + 1)/(e^E - 1)] \quad (16)$$

where (in SI units)

$$E = (2z_+^2e^2\sum n_+/\epsilon k_BT)^{1/2}\delta + \ln [(e^D + 1)/(e^D - 1)] \quad (17)$$

where $D = z_+e\psi_0/2k_BT$, δ is the thickness of the Stern layer, and $\sum n_+$ is the total number concentration of the counterion. Following Ottewill et al.,[25] the surface potential (ψ_0) for particles of the size and surface charge density considered here can be estimated from

$$\psi_0 = 4\pi r_i\sigma/4\pi\epsilon(1 + \kappa r_i) \quad (18)$$

where σ is the surface charge density on the particle (SI units are again used). If the surface potential exceeds 50 mV, it is better to use the flat-plate expression

$$\psi_0 = (2k_BT/z_+e) \sinh^{-1} [2\pi z_+e\sigma/(4\pi\epsilon k_BT\kappa)] \quad (19)$$

For values of ψ_0 exceeding 50 mV, a smooth transition between eq 18 and 19 is achieved through use of a switching function.

The van der Waals attractive potential is given by

$$V_A(r_i,r_j,H) = -(A^*/6)[2/(s^2 - 4) + 2/s^2 + \ln [(s^2 - 4)/s^2]] \quad (20)$$

where $s = 2 + (H/r_{ij})$ and A^* is the effective Hamaker constant of the particles in the dispersion medium.

In the surfactant-free systems considered here, the surface charge density must arise solely from surface-active species generated by initiator decomposition. Not all of the primary free radicals, however, necessarily grow to precursor particles or enter mature latex particles. This provides a reservoir of surfactant generated in situ in the aqueous phase, even in the absence of added emulsifier. It is necessary at this juncture to take account of the adsorption isotherm of these species, since many will be of low molecular weight. It is sufficient for this purpose to adopt the Langmuir adsorption isotherm

$$N_s = \frac{A_t}{a_s(1 + b^{-1}[S_w]^{-1})} \quad (21)$$

Here N_s is the total number of surface sites occupied by surface-active species, A_t is the total area of precursors plus latex particles (both of these quantities refer to unit volume of reacting mixture), $[S_w]$ is the concentration of the surface-active species in the aqueous phase, a_s is the area occupied by a surface-active species when close-packed, and b is a constant depending on the surfactant and surface. If $[S_t]$ is the total amount of surface-active species present (adsorbed or in solution) per unit volume of the aqueous phase, then

$$[S_t] = (N_s/N_A) + [S_w] \quad (22)$$

Combining eq 21 and 22 then yields for $[S_w]$

$$[S_w] = (U^2 + [S_t]b^{-1})^{1/2} - U \quad (23)$$

where $U = {}^1/_2[b^{-1} + A_t(N_Aa_s)^{-1} - [S_t]]$. Assuming that all precursors have the same surface charge density, we have

$$\sigma = e/[a_s(1 + b^{-1}[S_w]^{-1})] \quad (24)$$

The total concentration of surface-active agent $[S_t]$ (produced solely from initiator decomposition in the emulsifier-free systems considered here) at time t will be given by

$$[S_t] = 2k_dC_It \quad (25)$$

while the total area of precursors plus latex is given by

$$A_t = \sum 4\pi r_j^2Y_j \quad (26)$$

Equations 21–26 together give the required expression for the surface charge density. Note that eq 25 assumes that all primary free radicals are available to be incorporated into the surfaces of the latex particles; this does not imply that the radical capture efficiencies are 100%, because charged end groups may well be incorporated into the particles as surface-active species formed in the aqueous phase that are not free radical in character.

Many features incorporated in the present model have been used by Fitch and co-workers[26] in an extension of HUFT theory. However, their work did not take account of the special features of heterocoagulation and also omitted the effect of coagulation of particle growth (instead of treating coagulation only in terms of loss of free radical activity). The contribution of coagulation to particle growth, as set out in eq 1 and 2, is an essential feature of the present model.

Solution of Coagulative Nucleation Equations

Equations 1–3, 5, 6, and 8–26 constitute the requisite set of evolution equations describing the coagulative nucleation mechanism. Their complexity is such that it is necessary to resort to a numerical solution (although it may be possible in the future to make sufficient approximations under certain circumstances so that analytical solutions could be obtained). The numerical solution is less than straightforward, because of the large number of equations and their numerical instability. The following devices enable solutions to be readily and economically generated by using standard methods for the solution of differential equations (such as the Gear algorithm).

(1) One notes that primary precursors are expected to be relatively large (typically a few nanometers). If they were composed of a single polymer molecule, this size would correspond to a high degree of polymerization (10^2–10^3). Thus the number of equations (values of P) in eq 5 could well be huge. This difficulty is readily overcome by resorting to the continuum version, eq 7, expressed as finite difference equations (i.e., choosing some grain size Δ, consisting say of 100 monomer units). Taking note that one should treat the first oligomer separately, the finite difference equations are

$$dy_1/dt = 2k_dC_I - k_pC_wy_1 - y_1Z \quad (27)$$

$$dy_P/dt = \Delta^{-1}(q_{P-1}y_{P-1} - q_Py_P) - y_PZ, \qquad P \geq 2 \quad (28)$$

where

$$Z = k_t(y_1 + \Delta\sum_{j>1} y_j) + \sum B_{Pj}Y_j \quad (29)$$

and $q_P = k_p C_M^P$. The special case of primary free radicals ($P = 1$) has been specifically incorporated into eq 27, where C_w is the aqueous phase monomer concentration. The rate of creation of primary precursors is then

$$g(t) = q_J y_J/\Delta \quad (30)$$

Equations 27–30 can now be easily and accurately solved as a comparatively small number of ordinary differential equations for a suitable choice of Δ.

(2) The monomer concentration in a precursor of volume V_j, C_M^j, can in principle be determined from the equation of Morton et al.[27] (based in part on the Flory–Huggins theory). However, the values of the parameters to be used therein (and, indeed, even the validity of the equation itself) are uncertain. One means of overcoming this problem has been presented by Fitch et al.;[26] we here present an alternative procedure. We note that the main result of this equation is that, for small radii, C_M is an increasing function of radius. Further, it is unlikely that the final particle number will be strongly dependent on the precise functional form for $C_M(r)$. We therefore adopt the following form, which although somewhat arbitrary, is in qualitative accord with the Morton equation and also approaches the aqueous-phase concentration (C_w) for very small particle radii:

$$C_M(r) = C_M^\infty \tanh(r/r_{FH}), \quad r > r^*$$
$$= \exp[\ln(C_w) + (r/r^*)^3 \ln[C_M(r^*)/C_w]], \quad r \geq r^* \quad (31)$$

where C_M^∞ is the large-radius-limiting saturated monomer concentration in the particles, r_{FH} is a radius chosen to express the Flory–Huggins parameters (see below), and r^* a radius sufficiently small that one expects the value of C_M to be governed by oligomer-like rather than particle-like considerations. Numerical tests show that physically reasonable alternative empirical expressions for $C_M(r)$ do not lead to significant changes in final particle number.

(3) Similar uncertainties exist for the monomer concentration in a P-meric oligomer. As pointed out above, C_M^P must range from C_w for $P = 1$ through to C_M^1 (that in a primary precursor) for $P = J$. Quantitative prediction of this variation is a particularly difficult thermodynamic problem, since the particles will clearly not be spherically symmetric in shape, nor will there be a sharp interface between the particle and the aqueous phase. Since the degree of polymerization of the oligomer(s) in a primary precursor will be comparatively high, we assume here that eq 31 also holds for oligomers; we note that this form was chosen to give the correct limiting behavior of C_M for large and small sizes of the entity concerned.

(4) Equations 1–3 and 8–31 now give the required set of ordinary differential equations for the particle number etc. These equations are highly nonlinear through a number of terms, principally the second-order terms such as $B_{ij}Y_iY_j$ and, even more importantly, through the strong dependence of the B_{ij} on the ζ-potentials. The latter are themselves strong functions of the populations through eq 8–26. This nonlinearity can readily introduce numerical instabilities. For example, the Y_j's for larger j are initially zero and can easily assume small negative values in the first few integration steps because of numerical error; these nonphysical values can subsequently become quite large because of the ill-conditioned nature of the equations. In numerical integration it is therefore essential to use a tight error criterion and, if necessary, to reset any spurious negative concentrations to zero.

(5) Numerical instabilities can be enhanced by some choices of initial conditions: it can be seen from the foregoing discussion that the physically correct starting condition requiring all y_P and Y_j to be zero will be especially prone to this. This problem is overcome by choosing initial conditions such that all the y_P except for the higher P have their steady-state values (with y_P for higher P and all the Y_j initially set to zero); the concentrations then adjust themselves to their correct non-steady-state values in the first integration step, without error propagation. Inaccuracies can arise if it is assumed that the y_P *always* have their steady-state values (as is done in the conventional application of HUFT theory); their (non-steady-state) time evolution should be included in the differential equations, as described above.

(6) The initial value for the surface charge density σ is undefined at $t = 0$ in eq 24, since $[S_w]$ is initially zero in a surfactant-free system. This problem can be overcome by setting its initial value to that corresponding to an integral number (say, 1 or 2) of charged species per primary precursor (as suggested by Ottewill and co-workers[25]). Thus, for primary precursors, we set $\sigma(t=0) = ne/4\pi r_P^2$, where n is the number of charged groups, and for other precursors, the initial surface charge density is (r_i/r_P) times that on a primary precursor. The surface charge density is then allowed to evolve in time as dictated by eq 1–3 and 8–31, subject to the following constraint. Early-time instabilities can be prevented by ensuring that σ does not go below the $t = 0$ value (a constraint which is quite reasonable physically). When the numerical integration is performed with this constraint, it is found that σ evolves smoothly in time and that the final N_c is insensitive to the choice of the initial number of charged groups per primary precursor.

Calculations on Surfactant-Free Systems

In all calculations reported here, the following parameter values were chosen. The value of k_p was taken as 480 dm^3 mol^{-1} s^{-1};[28] k_d was 2.3×10^{-5} s^{-1};[29] C_M^∞ was 5.8 mol dm^{-3} (actually applicable to styrene at 50 °C,[28] as no data are available for 70 °C; this should not introduce serious errors). The value of k_t for eq 27–29 was chosen as 10^6 dm^3 mol^{-1} s^{-1}; this is a reasonable value for termination between polymer chains of degree of polymerization ca. 10^2–10^3 at low dilution by monomer.[30] The primary precursor radius was chosen as 2 nm, although the results do not change strongly if r_P is varied over the range 1–2.5 nm.

The average number of free radicals per precursor and latex particle ($\bar{n}$) was chosen as follows. For small particles, where exit (desorption) is likely to be important,[28] $\bar{n}$ is expected to be appreciably less than $^1/_2$. Under these conditions,[28] $\bar{n} \triangleq \rho/k$, where ρ is the rate coefficient for entry of free radicals into the particles and k is that for exit. For low particle numbers such as found in these systems, the initiator efficiency will be low, and so it is expected that ρ would be approximately proportional to $C_I^{1/2}$. The actual values of ρ and k depend on the aqueous phase and intraparticle kinetics,[28] and the a priori calculation of ρ and k requires a knowledge of some rate parameters whose values are at present uncertain in the systems under consideration. For simplicity, we assume that $\bar{n} \propto C_I^{1/2}$ and is independent of precursor volume, with the proportionality factor chosen to give $\bar{n} = 0.1$ for the lowest initiator concentration considered here (2.76×10^{-4} mol dm^{-3}); this is in accord with experimental values of $\bar{n}$ for styrene in seeded systems at 50 °C under similar conditions.[28] Calculations show that the final particle

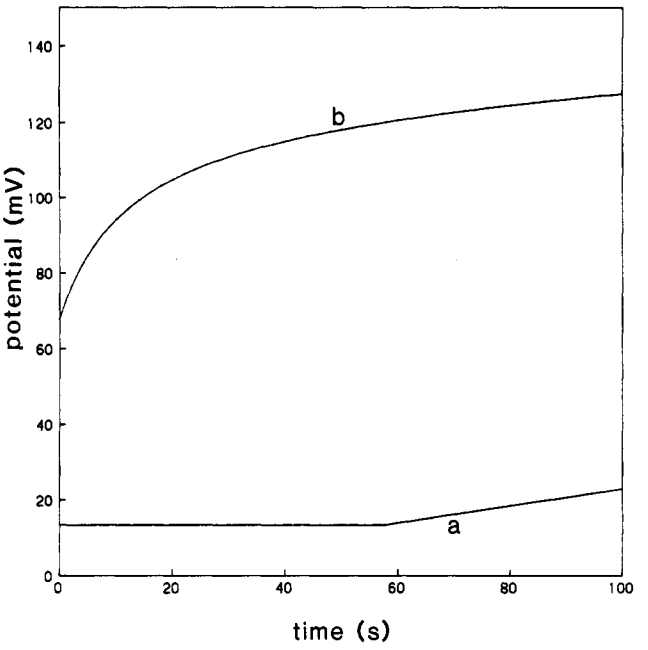

Figure 1. Surface potentials as function of time for primary precursor (a) and for latex particles (b), for a styrene system with initiator concentration $C_I = 2.76 \times 10^{-3}$ mol dm^{-3}, ionic strength $I = 8.28 \times 10^{-3}$ mol dm^{-3} (no added electrolyte apart from initiator), and other parameters as described in the text.

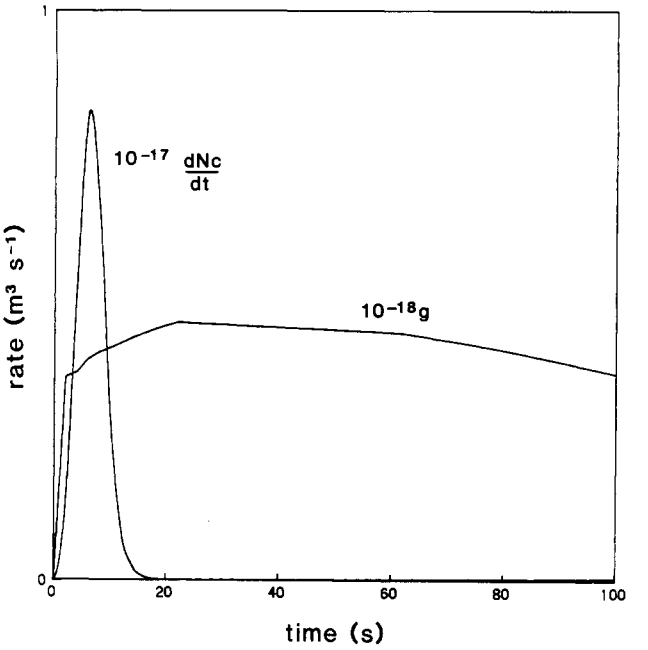

Figure 2. Rates of formation of primary precursors, $g(t)$, and of latex particles, dN_c/dt, as functions of time t, calculated for the system of Figure 1.

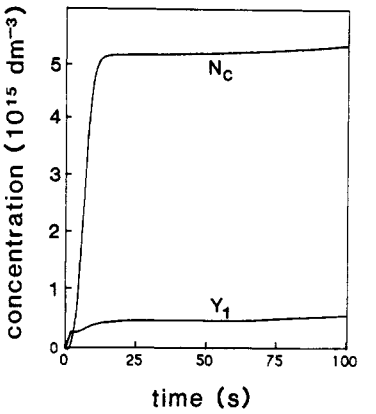

Figure 3. Number concentrations of primary precursors $[Y_1(t)]$, and of latex particles $[Y_m(t) \equiv N_c(t)]$ as functions of time, calculated for the system of Figure 1.

number is not strongly sensitive to the value assumed for $\bar{n}$: e.g., changing $\bar{n}$ by a factor of 3 typically changes N_c by 50%. (It should be noted that on the other hand the particle size *distribution* is a strong function of $\bar{n}$.)

The adsorption isotherm parameters a_s and b were chosen to be those found by Ahmed et al.[31] for sodium dodecyl sulfate on polystyrene at 25 °C, viz., $a_s = 43$ Å^2 and $b = 2.4 \times 10^3$ dm^3 mol^{-1} (the final N_c values are insensitive to b). A value of 15 nm was chosen for r_{FH}: this implies that the precursors will have an equilibrium monomer concentration C_M equal to half the large-radius limiting value at $r = 15$ tanh^{-1} $^1/_2 \triangleq 8$ nm. A value of 1 nm was chosen for r^*: that is, we assume that the Morton equation becomes qualitatively inappropriate below this size and that at very small radii C_M exponentially approaches the value expected for monomer in water (viz., C_w). Results are not sensitive to the values of r_{FH} and r^* (over a physically reasonable range). It should be noted that the foregoing values for these quantities are quite empirical (although they do not contradict physical intuition) and that experimental information on monomer swelling of very small particles and oligomers (e.g., by neutron diffraction) is an important area for future research. The thickness of the Stern layer (δ) was taken to be 0.141 nm (the "diameter" of a water molecule). The effective Hamaker constant A^* for polystyrene was taken to be[32] 5×10^{-21} J.

The term Z in eq 27–29 requires the entry rate coefficient for oligomers into precursors. For simplicity, we replace the term $\sum B_{Pj} Y_j$ by $k_e \sum Y_j$, where k_e is an average entry rate coefficient. This last quantity is subject to some uncertainty. Measurements of k_e for styrene latex particles at 50 °C at high concentrations of surfactant yield values of ca. 10^5–10^6 dm^3 mol^{-1} s^{-1}.[33] Now, the rate of coagulation of a small precursor with a large latex particle, as calculated either from the Healy–Hogg expressions or from the theory of Barouch et al., is found to be some orders of magnitude more than the experimentally observed[33] k_e. This suggests that entry of oligomers is controlled by processes other than simple colloidal diffusion and that additional steps such as coalescence of the oligomer into the interior of the particle may be involved. If so, the latter step would clearly be a function of the monomer concentration in the latex particles. We adopt the heuristic assumption that $k_e(r) = k_e^\infty [C_M(r)/C_M^\infty]$. Values of k_e^∞ in the range of 10^6–10^8 dm^3 mol^{-1} s^{-1} were used, the higher value being the lower bound of B_{1m} in the present system (note that no data on k_e in surfactant-free systems are available). A value of k_e^∞ of 10^8 dm^3 mol^{-1} s^{-1} was used in the results reported here.

Results and Discussion

Theoretical Predictions. Figures 1–4 show some typical results from calculations of particle nucleation kinetics for the conditions used by Ottewill and co-workers on surfactant-free styrene emulsion polymerization.[10] These illustrative examples are for a temperature of 70 °C, an initiator concentration $C_I = 2.76 \times 10^{-3}$ mol dm^{-3}, and no additional electrolyte.

Figure 1 shows the calculated surface potentials as functions of time, for primary precursors and for mature latex particles. Precursors are initially unstable with regard to homocoagulation: the values of the surface potential at early times yield homocoagulation rate coeffi-

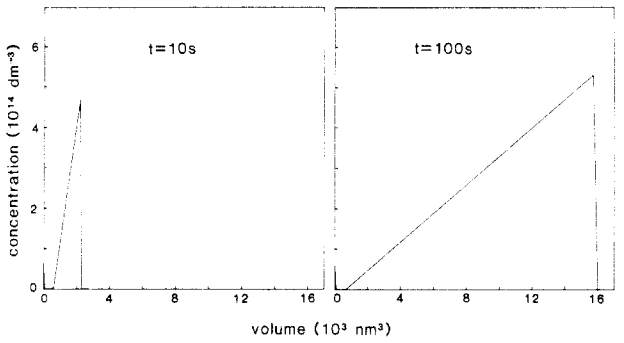

Figure 4. Calculated particle size distributions for the system of Figure 1, for t = 10 and 100 s. Concentrations of latex particles ($Y_m \equiv N_c$) are calculated for a single (but time-dependent volume) V_m and thus are represented as spikes.

cients close to the diffusion limit. Homocoagulation of precursors is slower at late times than at early times, due partly to increases in surface potential and partly to increases in radius. For particles of comparable size and surface potential, colloidal stability is a function both of surface potential and of radius (increasing with increasing values of both parameters). Both the radius and surface potential conspire to make primary precursors unstable to homocoagulation, whereas large particles are stable. The surface potential for the larger particles is seen to be always significantly greater than that for the primary precursors, and the values of B_{mm} calculated from these surface potentials show that larger particles are indeed colloidally stable.

These effects are also manifest in the time dependences of the rate of creation of primary precursors, $g(t)$, and of latex particles, dN_c/dt, shown in Figure 2. The former shows a gradual decrease at later times because of the effect of entry into particles (and precursors), i.e., of the $\sum Y_j$ term in the Z of eq 27–29. This is of course in accord with the HUFT theory (since it contains the HUFT theory within it).

The time dependence of dN_c/dt, the rate of particle formation, shown in Figure 2 shows a rapid increase followed by a somewhat slower decrease. This calculated result for the present emulsifier-free systems is qualitatively in accord with the forms of dN_c/dt deduced from the time evolution of particle size distributions in systems containing surfactant.[12] The present surfactant-free systems, however, show a more rapid rise than that in surfactant-containing systems because coagulation is quicker in the complete absence of added stabilizer. Further, particle number densities in these systems plateau at significantly lower values than in the presence of added surfactant, thus shortening the nucleation period.

Figure 3 shows the populations of primary precursors and of mature particles as functions of time; these follow the rates displayed in Figure 2 [although note that dY_1/dt contains loss terms as well as the gain term $g(t)$]. The population of primary precursors shows an initial rapid rise as they are created from oligomers. This population then approaches a limiting value at later times.

Figure 4 shows the predicted time evolution of the particle size distribution (PSD) for precursors, i.e., the concentrations Y_j as functions of V_j. Because for computational simplicity we lump all stable particles together as Y_m, the width and skewness of the PSD of stable particles do not come directly from this calculation (although they can be readily computed from the dN_c/dt[12]), and thus the number concentration of these stable particles appears as a spike. Naturally, the treatment given in the present paper could be used to generate a full PSD by carrying out

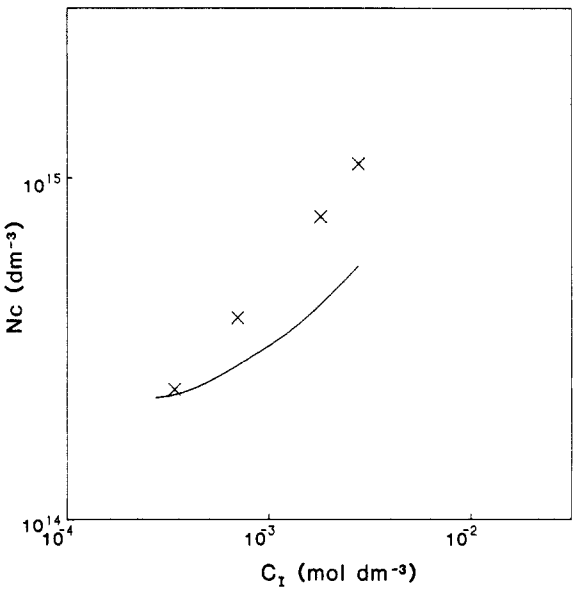

Figure 5. Calculated (line) and experimental[9,10] (points) final particle number densities (N_c) as functions of initiator concentration, for conditions described in the text.

the calculations for larger values of m (which it will be recalled is not so much the degree of coagulation of a stable particle as a quantity of convenience in the numerical simulations). Of particular interest in Figure 4 is the prediction that the PSD of precursors plus latex particles should be *bimodal*: significant concentrations of primary precursors are present. Such a prediction is again subject to experimental test, although it requires the measurement of PSDs by methods such as neutron scattering which are able to detect very small (ca. 2–5 nm) particles.

Comparison with Experimental Results. Varying Initiator Concentration. Figure 5 shows the predicted and experimental[10] dependences of the final number of latex particles (N_c) formed at 70 °C in a surfactant-free system as a function of C_I, with the ionic strength held constant at 1.13×10^{-2} mol dm^{-3}. Although the theoretical log/log plot of N_c against C_I is slightly curved, it can be least-squares fitted by

$$\log (N_c/\text{dm}^{-3}) = 15.7 + 0.4 \log (C_I/\text{mol dm}^{-3})$$

This may be compared with the experimental dependence reported by Goodwin et al.[9,10] (which we have here converted from the reported particle diameter dependence to a particle number dependence):

$$\log (N_c/\text{dm}^{-3}) = 16.9 + 0.72 \log (C_I/\text{mol dm}^{-3})$$

Clearly, the coagulative nucleation theory is moderately successful in predicting both the sizes of the latex particles formed and the dependence of the particle number on initiator concentration.

Varying Ionic Strength. Figure 6 compares the predicted and experimental[10] dependences of final particle number on ionic strength I, the initiator concentration being held constant at 2.76×10^{-3} mol dm^{-3}. Conditions are otherwise as for Figure 5. The theoretical dependence (when least-squares fitted to a straight line) obeys

$$\log (N_c/\text{dm}^{-3}) = 13.0 - 0.9 \log (I/\text{mol dm}^{-3})$$

The data of Goodwin et al.[9,10] fit the relation

$$\log (N_c/\text{dm}^{-3}) = 13.5 - 0.7 \log (I/\text{mol dm}^{-3})$$

Again, both the magnitude and dependence upon ionic strength are reproduced quite acceptably by coagulative

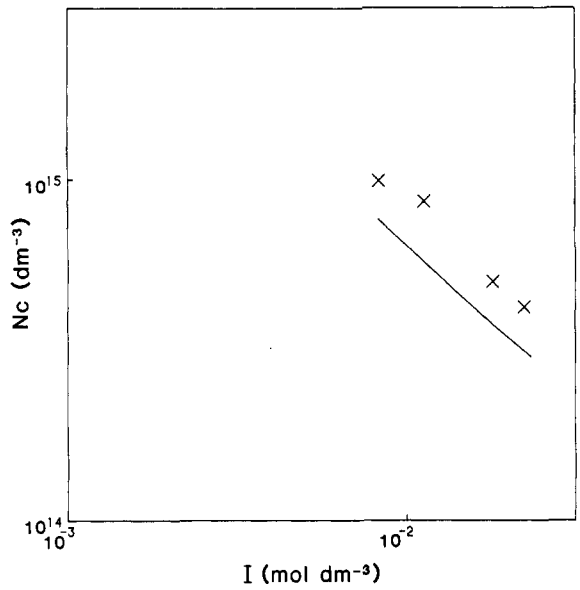

Figure 6. Calculated (line) and experimental[10] (points) final particle number densities (N_c) as functions of ionic strength, for conditions described in the text.

nucleation theory. It is noteworthy that the agreement is both qualitative and quantitative: the coagulative nucleation mechanism successfully reproduces the decrease of particle number with ionic strength and the increase with initiator concentration and, most importantly, the fact that the particle number in emulsifier-free systems is orders of magnitude lower than in ones containing normal amounts of added surfactant.

The comparison made above shows that there is agreement between experiment and the predictions of coagulative nucleation theory for surfactant-free systems. The results are all the more compelling in that the basic model was deduced from data for emulsifier-containing systems, wherein the particle number is typically 2 or 3 orders of magnitude greater than in the ones under study. The comparatively small discrepancies can be ascribed to inadequacies of DLVO theory and semiempirical evaluation of the coagulation rate coefficients.

Last, we note that in the present publication, we have confined our attention to styrene, a monomer that is fairly insoluble in water. A useful test of the model discussed here would be to apply it to surfactant-free data for monomers that are much more soluble in water; excellent data on surfactant-free emulsion polymerization are available on two such monomers (methyl methacrylate[5] and vinyl acetate[34]).

Conclusions

The quantitative model for coagulative nucleation developed here enables the time evolution of the number of latex particles in an emulsifier-free system to be predicted (extensions to systems with added surfactant will be presented in a later publication). The model as implemented here contains a small number of adjustable parameters: k_t for the oligomeric species, the parameters r^* and r_{FH} giving the monomer concentration in oligomers and particles, and $\bar{n}$. Generally, however, the qualitative and quantitative agreement of the predictions of coagulative nucleation theory with the results of experiment is strong evidence for the overall validity of the model. In surfactant-free systems, oligomeric-free radicals apparently undergo homogeneous nucleation to eventually form precursor particles; these grow both by propagation and by coagulation, the latter being important at early times. Primary precursor particles are colloidally unstable because of the extreme curvature of their surfaces. These grow by coagulation and propagation until the radius of curvature and surface charge density have increased sufficiently to allow double-layer interactions to impart colloidal stability: mature latex particles are thus formed. Increasing the ionic strength decreases the colloidal stability of the precursor particles so that fewer (and larger) particles are formed. Increasing the initiator concentration also increases the ionic strength; this effect is, however, outweighed by the increase in the flux of free radicals. It would appear that the partial attraction predicted theoretically by Barouch and Matijevic[22] for the heterocoagulation of particles of different sizes and different surface potentials (although of the same sign) plays a key role in "switching off" nucleation and replacing it by entry into mature latex particles.

Experimental results obtained for surfactant-free systems provide a critical test of the validity of coagulative nucleation theory, since coagulation must be an important contributor to particle formation in these systems. The ability of this theory to provide a reasonable description of such systems (both qualitatively, in the low particle number, and quantitatively, in the dependence of N_c on C_I and I) engenders confidence in the application of the coagulative nucleation theory to conventional emulsion polymerizations, which involve added emulsifier and whose nucleation process is complicated by the possible intrusion of other particle-formation mechanisms.

Acknowledgment. We deeply appreciate the collaboration of Professors E. Barouch and E. Matijevic, who carried out the E_m calculations for heterocoagulation used in this work. Constructive and thoughtful comments by John Richards and John Congalidis of E. I. du Pont de Nemours and Co. are gratefully acknowledged. We also thank the Australian Research Grants Scheme for its financial support of these studies. P.J.F. was supported by a Commonwealth Postgraduate Research Grant.

Registry No. PhCH=CH$_2$, 100-42-5.

References and Notes

(1) Harkins, W. D. *J. Am. Chem. Soc.* **1947**, *69*, 1428.
(2) Smith, W. V.; Ewart, R. H. *J. Chem. Phys.* **1948**, *16*, 592.
(3) Priest, W. J. *J. Phys. Chem.* **1952**, *56*, 1077.
(4) Dunn, A. S.: Chong, L. C.-H. *Br. Polym. J.* **1970**, *2*, 49.
(5) Fitch, R. M.; Tsai, C. H. In *Polymer Colloids*; Fitch, R. M., Ed.; Plenum: New York, 1971; p 73.
(6) Hansen, F. K.; Ugelstad, J. *J. Polym. Sci., Polym. Chem. Ed.* **1978**, *16*, 1953.
(7) Hansen, F. K.; Ugelstad, J. In *Emulsion Polymerization*; Piirma, I., Ed.; Academic: New York, 1982; p 51.
(8) Kotera, A.; Furusawa, K.; Takeda, Y. *Kolloid. Z. Z. Polym.* **1970**, *239*, 677; *240*, 837.
(9) Goodwin, J. W.; Hearn, J.; Ho, C. C.; Ottewill, R. H. *Br. Polym. J.* **1973**, *5*, 347.
(10) Goodwin, J. W.; Hearn, J.; Ho, C. C.; Ottewill, R. H. *Colloid Polym. Sci.* **1974**, *252*, 464.
(11) Lichti, G.; Gilbert, R. G.; Napper, D. H. *J. Polym. Sci., Polym. Chem. Ed.* **1983**, *21*, 269.
(12) Feeney, P. J.; Napper, D. H.; Gilbert, R. G. *Macromolecules* **1984**, *17*, 2520.
(13) Feeney, P. J.; Napper, D. H.; Gilbert, R. G. *J. Colloid Interface Sci.* **1985**, *107*, 159.
(14) Goodall, A. R.; Wilkinson, M. C.; Hearn, J. In *Polymer Colloids II*; Fitch, R. M., Ed.; Plenum: New York, 1980; p 629.
(15) Ottewill, R. H. In *Emulsion Polymerization*; Piirma, I., Ed.; Academic: New York, 1982; p 1.
(16) Fuchs, N. *Z. Phys.* **1934**, *89*, 736.
(17) Buscall, R.; Ottewill, R. H. In *Polymer Colloids*; Buscall, R., Corner, T., Stageman, J., Eds.; Elsevier: London, 1985; p 141.
(18) Overbeek, J. Th. G. In *Colloid Science*; Kruyt, H. H., Ed.; Elsevier: Amsterdam, 1952; Vol. I, p 278.
(19) Hogg, R.; Healy, T. W.; Fuerstenau, D. W. *Trans. Faraday Soc.* **1966**, *62*, 1638.

(20) Wiese, G. R.; Healy, T. W. *Trans. Faraday Soc.* **1970**, *66*, 490.
(21) Chan, D. Y. C.; White, L. R. *J. Colloid Interface Sci.* **1980**, *74*, 303.
(22) Barouch, E.; Matijevic, E. *J. Chem. Soc., Faraday Trans. 1* **1985**, *81*, 1797.
(23) Barouch, E.; Matijevic, E.; Wright, T. H. *J. Chem. Soc., Faraday Trans. 1* **1985**, *81*, 1819.
(24) Reerink, H.; Overbeek, J. Th. G. *Discuss. Faraday Soc.* **1954**, *18*, 74.
(25) Goodwin, J. H.; Ottewill, R. H.; Pelton, R.; Vianello, R.; Yates, D. E. *Br. Polymer J.* **1978**, *10*, 173.
(26) Fitch, R. M.; Palmgren, T. H.; Aoyagi, T.; Zuikov, A. *Angew. Makromol. Chem.* **1984**, *123/4*, 261.
(27) Morton, M.; Kaizerman, S.; Altier, M. W. *J. Colloid Sci.* **1968**, *6*, 2859.
(28) Gilbert, R. G.; Napper, D. H. *J. Macromol. Sci., Rev. Macromol. Chem. Phys.* **1983**, *C23*, 127.
(29) Kolthoff, I. M.; Miller, I. K. *J. Am. Chem. Soc.* **1951**, *73*, 3055, 5188.
(30) Ballard, M. J.; Napper, D. H.; Gilbert, R. G.; Sangster, D. F. *J. Polym. Sci., Polym. Chem. Ed.* **1986**, *24*, 1027.
(31) Ahmed, S. M.; El-Aasser, M. S.; Micale, F. J.; Poehlein, G. W.; Vanderhoff, J. W. In *Polymer* Colloids *II*; Fitch, R. M.; Ed.; Plenum: New York, 1980; p 265.
(32) Ottewill, R. H.; Walker, T. *J. Chem. Soc., Faraday Trans. 1* **1974**, *70*, 917.
(33) Penboss, I. A.; Gilbert, R. G.; Napper, D. H. *J. Chem. Soc., Faraday Trans. 1* **1986**, *82*, 2247.
(34) Nomura, M.; Sasaki, S.; Harada, M.; Eguchi, W. *J. Appl. Polym. Sci.* **1978**, *22*, 1043.

Semiempirical Determination of Solution Structure in Polymer Solutions Based on the Clustering Theory

S. Saeki,* M. Tsubokawa, and T. Yamaguchi

Department of Polymer Engineering, Fukui University, Fukui 910, Japan.
Received March 26, 1987; Revised Manuscript Received May 29, 1987

ABSTRACT: The solution structure in polymer solutions polystyrene(PS)–toluene, PS–cyclohexane, natural rubber(NR)–benzene, poly(*n*-butyl acrylate)(PNBA)–toluene, and polyisobutylene(PIB)–*n*-pentane has been determined based on the clustering theory by Zimm and by Kirkwood and Buff, which is expressed by $G_{00}/\bar{v}_0 = -\phi_1\{\partial(a_0/\phi_0)/\partial a_0\}_{P,T} - 1$, where G_{00} is the clustering function of solvent, $\bar{v}_0$ is the partial molecular volume of solvent, a_0 is the activity of solvent, and ϕ_0 and ϕ_1 are the volume fraction of solvent and polymer, respectively. Values of $G_{00}/\bar{v}_0$ determined in this work are 0.54 for PS–toluene, 10.0 for PS–cyclohexane, 1.67 for NR–benzene, 0.13 for PNBA–toluene, and 5.0 for PIB–*n*-pentane. The volume or segment fraction activity coefficients of solvent for the polymer solutions are found to be expressed by using the clustering theory $a_0/\phi_0 = A_0(\phi_0 + \beta - 1)^{-\beta}$ for the infinite molecular weight of polymer, which is essentially equivalent with that of the Huggins–Miller–Guggenheim theory where A_0 and β are constants and β is defined by $1 + (G_{00}/\bar{v}_0)^{-1}$. It is also found that the equation of a_0/ϕ_0 obtained in this work explains the concentration dependence of the polymer–solvent interaction parameter.

Introduction

The Flory–Huggins theory is the most fundamental theory in investigating the thermodynamic properties of polymer solution where the polymer–solvent interaction parameter χ is assumed to be independent of concentration and inversely proportional to the absolute temperature of the solution.[1] Apart from the configurational entropy term of the chemical potential in the theory, the two main assumptions for the χ parameter have been modified through the experimental observation of the concentration dependence of the χ parameter and the lower critical solution temperature observed in most of the nonpolar polymer solutions.[1-6] New expressions of χ for temperature, pressure, and concentration in the corresponding states theory by Flory[7,8] and Patterson[9,10] predict the upper and lower critical solution temperatures and their pressure dependence[2-6,11-13] and concentration dependence on χ.[7,8,14] On the other hand, Koningsveld and Kleintjens[15] proposed a closed expression for χ with respect to polymer concentration, which is derived from the free-energy expression of the Flory–Huggins theory with a concentration-dependent function of the polymer–solvent interaction parameter.

The other assumption used in the Flory–Huggins theory is the random mixing approximation. One of the earliest attempts to include the effect of inhomogeneity on solution thermodynamics was that of Kirkwood and Buff.[16] Zimm[17,18] developed a simple relation between the activity coefficient and the solvent clustering function on the basis of the Kirkwood–Buff theory. Fixman[19] attempted to determine the free energy by using the concentration-dependent interacton potentials and radial distribution functions. Huggins[20] derived an equation for the additional entropy term to the combinatorial entropy resulting from the concentration dependence of the randomness of orientation. A correlation between the local composition and overall mean concentration has been proposed by Renuncio and Prausnitz[21] and Brandani.[22]

In this work, we have examined the random mixing approximation used in most polymer solution theories through determination of the clustering function $G_{00}/\bar{v}_0$ in the Kirkwood–Buff–Zimm theory. We have also discussed a semiempirical equation on the activity coefficient of solvent derived in this work on the basis of the Huggins–Miller–Guggenheim theory,[23-25] the Flory theory of corresponding states, and the Koningsveld and Kleintjens theory.[15]

Semiempirical Determination of Clustering Function Based on the Kirkwood–Buff–Zimm Theory

Zimm[17] has derived the clustering function based on the Kirkwood–Buff theory,[16] which is given by

$$G_{00}/\bar{v}_0 = kT\kappa/\bar{v}_0 - \phi_1\{\partial(a_0/\phi_0)/\partial a_0\}_{P,T} - 1 \qquad (1)$$

where κ is the isothermal compressibility of the system, $\bar{v}_0$ is the partial molecular volume, ϕ_i is the volume fraction of solvent (0) and polymer (1), a_0 is the activity of solvent, and k is the Boltzmann constant. In this calculation, we used two assumptions in determining $G_{00}/\bar{v}_0$ and the

0024-9297/87/2220-2930$01.50/0